Contents lists available at SciVerse ScienceDirect

Comptes Rendus Chimie

www.sciencedirect.com

Full paper/Mémoire

Functionalization of short multi-walled carbon nanotubes with creatinine and aromatic aldehydes via microwave and thermal methods and their influence on the MKN45 and MCF7 cancer cells

Hasan Tahermansouri *, Hosna Ghobadinejad

Department of Chemistry, Ayatollah Amoli Branch, Islamic Azad University, PO Box 678, Amol, Iran

ARTICLE INFO

ABSTRACT

The chemical functionalization of carboxylated short multi-walled carbon nanotubes (Sh–MWCNT–COOH) by creatinine (Sh–MWCNT–amide) and later modification with aromatic aldehydes for producing 2-amino-5-arylidene-1-methyl-1H–imidazol-4(5H)-one (Sh–MWCNT–imidazols) via thermal and microwave methods have been investigated. All the products were characterized by Fourier transform infrared spectroscopy, Raman spectroscopy, scanning electron microscope, elemental analysis, thermogravimetric analysis, derivative thermogravimetric and cellular investigations. These functionalizations have been chosen due to the active sites of C=C and carbonyl groups in Sh–MWCNT–imidazols, which might be used as functional materials in the future. MTT assay was used to examine the behavior of cell proliferation after 72 h of cell culture experiments. Cellular investigations were performed for two kinds of cells, human breast and gastric cancer cells. Cellular results showed high toxicity of modified Sh–MWCNTs on the gastric cancer cells compared to breast cells.

© 2013 Académie des sciences. Published by Elsevier Masson SAS. All rights reserved.

1. Introduction

The hollow cylindrical structures made of carbon atoms, in which carbon nanotubes (CNTs) are introduced, as one of the representative paradigms among nanostructured carbon materials, have attracted great attention in the field of molecular electronics, sensing, composite materials, and cancer therapy [1–3]. There are two main types of CNTs that are used most commonly: single-walled carbon nanotubes (SWCNTs) and multi-walled carbon nanotubes (MWCNTs). MWCNTs are more attractive than SWCNTs because of their relatively low production costs and availability in large quantities. Biomedical applications for MWCNTs are investigated actively because of their useful combination of size and physicochemical properties [4–6].

Functionalization of CNTs involves the generation of chemical moieties on their surface in order to modify their physical and chemical properties, leading to the improvement of their performance for specific applications. The functionalized carbon nanotubes (f-CNTs) are believed to be very promising in the field of biological technologies. For example, it has been confirmed that gene expression through f-CNTs levels were up to 10 times higher than those achieved with deoxyribonucleic acid (DNA) alone [7]. Also, it has been proposed that f-CNTs can also be used for drug delivery [8]. Thus, extensive researches have been focused on the functionalization of CNTs, among which we can cite cycloaddition [9], oxidation [10], acylation [11], and amidation [12–18]. Also, review articles have been dedicated to this topic [19,20]. Chemistry under microwave radiation is known to be somewhat different, faster, and more efficient than the conventional chemical methods (refluxing and sonication) which require accurate control of temperature, atmosphere, and reaction time [13,14,21] for functionalizing CNTs. However, in this

* Corresponding author.
  E-mail address: h.tahermansuri@iauamol.ac.ir (H. Tahermansouri).

Sh-MWCNT-Amide   **Sh-MWCNT-imidazols (1-3)**
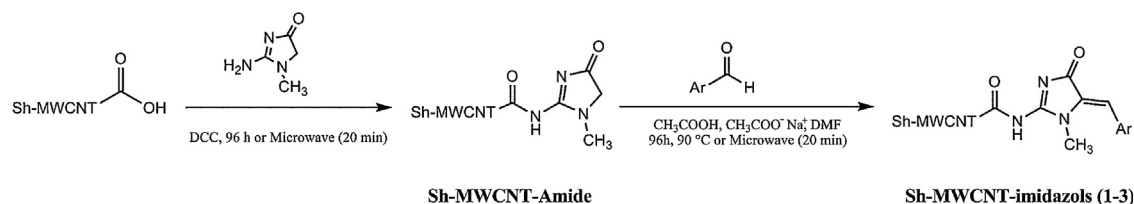
modified Sh-MWCNTs	Sh-MWCNT-imidazol(1)	Sh-MWCNT-imidazol(2)	Sh-MWCNT-imidazol(3)
Ar	⟨—◯—⟩H	⟨—◯—⟩OCH₃	HO⟨◯⟩

Fig. 1. Synthesis route to modified Sh–MWCNT–COOH with imidazol derivatives via thermal and microwave methods.

current study, in addition to developing Sh–MWCNTs amidation with creatinine, we have investigated the formation of 2-amino-5-arylidene-1-methyl-1H–imidazol-4(5H)-one (Sh–MWCNT–imidazols) on the carboxylated Sh–MWCNTs via thermal (refluxing) and microwave methods, with similar results. The products were characterized by Fourier transform infrared spectroscopy (FTIR), Raman, field emission scanning electron microscopy (FESEM), thermogravimetric analysis (TGA), derivative thermogravimetric (DTG) and elemental analysis. The route to the synthesis of modified Sh–MWCNT–COOH is displayed in Fig. 1.

Also, investigations about the toxicity of modified Sh–MWCNTs were performed on the cancer cells of human breast and gastric. Cellular results showed a high toxicity of modified Sh–MWCNTs on gastric cancer cells compared to that on breast cells.

2. Experimental

2.1. Materials and characterization

All the reagents and solvents, such as creatinine, benzaldehyde, 4-methoxy benzaldehyde, 2-hydroxy benzaldehyde, dicyclohexylcarbodiimide (DCC), tetrahydrofuran (THF) and dimethylformamide (DMF) have been purchased from Merck Chemical Inc. and short-MWCNTs–COOH (%95 purity, OD: 10–20 nm, length: 0.5–2 μm, content of COOH groups: 2 wt %, Netvino Co., Ltd) have been used as received. The experiments were carried out in an Ethos Model microwave oven (Milestone Co., Ltd.) with a 100-mL reaction chamber, which was lined with Teflon PFA and fitted with a 0–100 bar pressure controller. The FTIR spectrum was recorded using KBr tablets on a Thermo Nicolet Nexus 870 FTIR spectrometer. Raman spectra were recorded on an Almega Thermo Nicolet Dispersive Raman Spectrometer (532 nm of a Nd:YLF laser). FESEM was used to study the morphology of the MWCNTs. FESEM measurements were carried out on a Hitachi S4160 (Cold Field Emission) Electron Microscope. Elemental analyses of C, H, N were performed with a PerkinElmer (USA) 2400

Series II CHNS/O Elemental Analyzer. The samples were studied by thermogravimetric analysis (Netzsch TG 209 F1 Iris®) under nitrogen gas atmosphere (10 °C/min).

2.2. Preparation of Sh–MWCNT–amide with microwave method

An amount of 100 mg of the Sh–MWCNT–COOH was mixed with 200 mg of creatinine and then was sonicated in 30 mL of DMF for 15 min. Subsequently, the mixture was loaded into an extraction vessel. The microwave power and pressure was set to 800 W and 8 bar, respectively, and the reaction was carried out for 20 min. After cooling to room temperature, the mixture was filtered and washed thoroughly with DMF, ethyl alcohol and THF. Thus, the black solid was vacuum dried at room temperature for 15 h.

2.3. Preparation of Sh–MWCNT–imidazols with microwave method

An amount of 50 mg of Sh–MWCNT–amide was sonicated in 15 mL of DMF and then the mixture of 10 mmol of the aromatic aldehyde and 10 mL of a buffer solution (made of 10 mL of acetic acid and 0.2 g of sodium acetate) was added to the reaction mixture and was submitted to microwave irradiation (800 W) for 20 min. After cooling to room temperature, the reaction mixture was separated by centrifugation and washed thoroughly with THF and ethyl alcohol. Thus, the obtained solid was dried under vacuum for 15 h.

2.4. Preparation of Sh–MWCNT–amide with thermal method

An amount of 100 mg of the Sh–MWCNT–COOH was thoroughly dispersed in 30 mL of DMF by sonication. To this dispersion of Sh–MWCNT–COOH, 10 mL of the DMF solution in which 200 mg of creatinine had been dissolved was added. Then, 10 mL of THF solution of an excess amount of dicyclohexylcarbodiimide (DCC) was added to this solution dropwise; the mixture was further stirred at room temperature for 96 h, then filtered and washed thoroughly with DMF, ethyl alcohol and THF.

Subsequently, the black solid was dried at room temperature for 15 h under vacuum.

2.5. Preparation of Sh–MWCNT–imidazols with thermal method

An amount of 50 mg of the Sh–MWCNT–amide was sonicated in 10 mL DMF for 15 min to give a homogeneous suspension. Then, the mixture of 10 mmol of aromatic aldehyde and 10 mL of buffer (made of 10 mL of acetic acid and 0.2 g of sodium acetate) was added to the reaction mixture, which was then stirred at 90 °C for 96 h. After cooling to room temperature, the reaction mixture was separated by centrifugation and washed thoroughly with DMF, ethyl alcohol, and THF. Thus, the obtained solids were vacuum dried for 15 h.

2.6. Cellular study

2.6.1. Materials

The following substances were obtained from the sources as indicated. The cell culture medium (RPMI1640), fetal calf serum, 0.25% trypsin with 1 mM of ethylene diamine tetraacetate (EDTA), streptomycin sulfate, and penicillin G sodium were all obtained from GIBCO (Grand Island, NY, USA). Human gastric cancer cell line MKN45 (NCBI No: C615) and human breast cancer cell line MCF7 were provided by the Iranian Pasteur Institute Cell Bank (Tehran, Iran).

2.6.2. Cell culture

MKN45 or MCF7 was cultured in RPMI1640 supplemented with 10% of fetal bovine serum and 1% of L-glutamine, penicillin, and streptomycin. For these experiments, the cells were seeded at a density of 1×10^5 cells/mL in 96-well plates. At least three time points are depicted for each assay.

2.6.3. Cell proliferation

The MTT assay (Sigma) was used to evaluate the proliferative activity. Cells grown in 96-well plates were exposed to Sh–MWCNTs–COOH and modified Sh–MWCNTs. Exposure to 50 μL of RPMI1640 was used as a negative control and to 50 μL of dimethyl sulfoxide as a positive control. After 48 h, 20 μL of a 3-(4,5-dimethyl-2-thiazolyl)-2,5-diphenyl-2H-tetrazolium bromide (MTT) solution at 0.5 mg/mL in a Hank's balanced salt solution was added to each well and incubated for 4 h. Afterward, 150 μL of the MTT solution (10% Triton X-100 in 0.1 N HCl in anhydrous isopropanol) was added to each well. The resulting formazan crystals were solubilized in acidic isopropanol and quantified by measuring the absorbance at 570 nm with microplate reader (Rayto RT-6100). Data were calibrated using the appropriate calibration curve, as stated in Sigma protocols.

2.6.4. Statistics

All data were collected using Microsoft Excel®. Graphs and statistics were performed with SPSS11.5. Continuous variables were presented as mean ± SD ($x \pm s$). Data were analyzed using a one-way ANOVA to determine the difference among groups. Relative grown rates (RGR) of cells were calculated using the formula:

RGR = OD of each group/OD of natural group × 100%

To determine the cytotoxic response of the Sh–MWCNTs to cultured cells, 6-graded toxicity and other analytic methods were used.

3. Results and discussion

Fig. 1 illustrates the procedure for the functionalization of Sh–MWCNT–COOH by creatinine and aromatic aldehydes. The functionalized CNTs were characterized by elemental analysis, FESEM, FTIR, TGA, DTG and Raman spectroscopy. Elemental analyses of the modified Sh–MWCNTs are shown in Table 1. Apart from the carbon values, the changes of the atomic percentages of H (1.16%) and N (4.32%) in Sh–MWCNT–amide, and H (1.37%), N (3.45%) in Sh–MWCNT–imidazol (**1**), H (1.58%) and N (3.21%) in Sh–MWCNT–imidazol (**2**), H (1.29%) and N (3.32%) in Sh–MWCNT–imidazol (**3**) (compared to those in Sh–MWCNT–COOH) indicate that Sh–MWCNT–COOH is functionalized. On the other hand, the increase of the H percentage in Sh–MWCNT–imidazols **1**–**3** compared to Sh–MWCNT–amide confirms the formation of imidazol derivatives on the MWCNTs. Based on these data, coupled with the assumption that the atomic percentages of nitrogen and hydrogen originate from the employed creatinine and aromatic aldehydes, we confirmed the functionalization of Sh–MWCNT–COOH.

More evidence for the functionalization of Sh–MWCNTs was obtained by FESEM images. In Fig. 2, FESEM images of modified Sh–MWCNTs are shown. In the SEM image of Sh–MWCNT–COOH, it seems that the uniform surfaces of nanotubes are relatively smooth. On the other hand, for the Sh–MWCNT–amide and Sh–MWCNT–imidazols (**1**–**3**), a tubular layer of uniform organic compounds (creatinine and imidazole derivatives) is clearly present on the surface of the MWCNT (the rough part), and their diameters are slightly increased as compared to that of Sh–MWCNT–COOH. It may be due to covalently bonded creatinine and imidazol derivatives on the surface of the MWCNT as compared to that of Sh–MWCNT–COOH. These structures, Sh–MWCNT–amide and Sh–MWCNT–imidazols (**1**–**3**), are quite different from those of the starting Sh–MWCNT–COOH, as depicted in Fig. 2.

Fig. 3 presents the FTIR spectrum of modified Sh–MWCNTs. In Sh–MWCNTs–COOH, the peak at 1579 cm^{-1} is assigned to the active carbon stretching mode of the Sh–MWCNT–COOH [12] that forms the framework of the carbon nanotube sidewall. The appearance of the absorp-

Table 1
Elemental analysis of modified Sh–MWCNTs.

Sh–MWCNTs	% C	% H	% N
Sh–MWCNT–COOH	93.43	0.62	0.00
Sh–MWCNT–amide	89.74	1.16	4.32
Sh–MWCNT–imidazol (**1**)	90.36	1.37	3.45
Sh–MWCNT–imidazol (**2**)	88.56	1.58	3.21
Sh–MWCNT–imidazol (**3**)	88.61	1.29	3.32

Sh–MWCNTs: short multi-walled carbon nanotubes.

Sh-MWCNT-COOH   **Sh-MWCNT-Amidc**   **Sh-MWCNT-imidazol(1)**

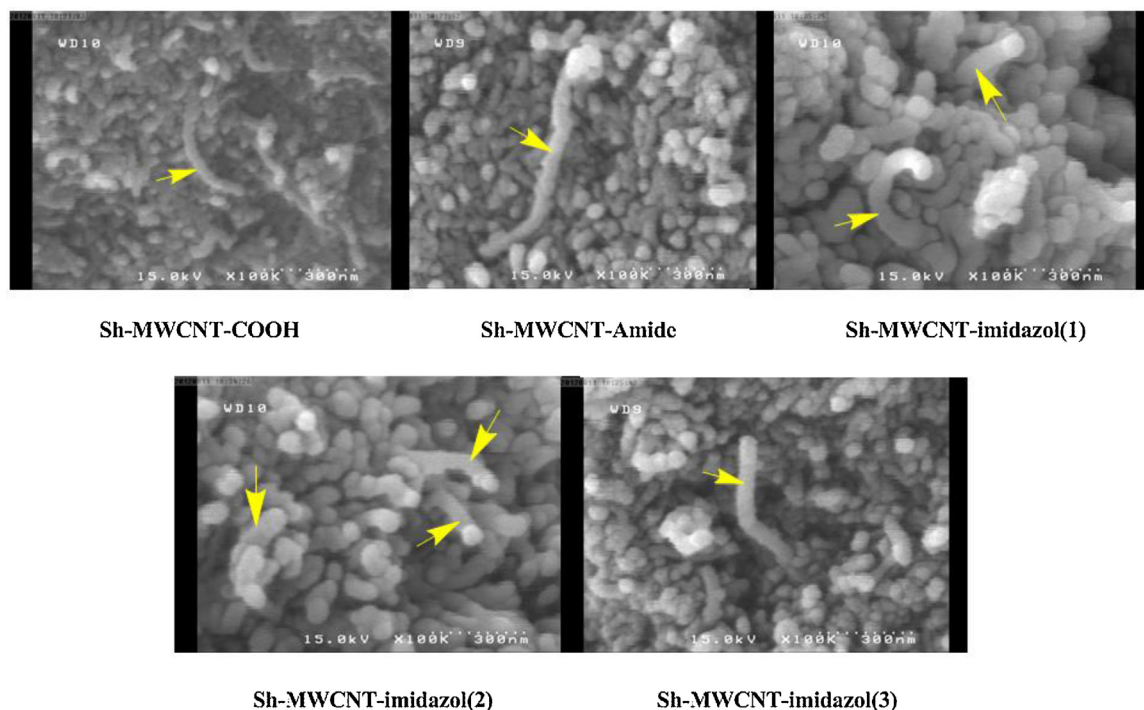**Sh-MWCNT-imidazol(2)**   **Sh-MWCNT-imidazol(3)**

Fig. 2. FESEM images of modified Sh–MWCNTs. The yellow arrows in Sh–MWCNT–amide and Sh–MWCNT–imidazols show a slight thickness increase on the surface of tubes compared to the case of Sh–MWCNT–COOH.
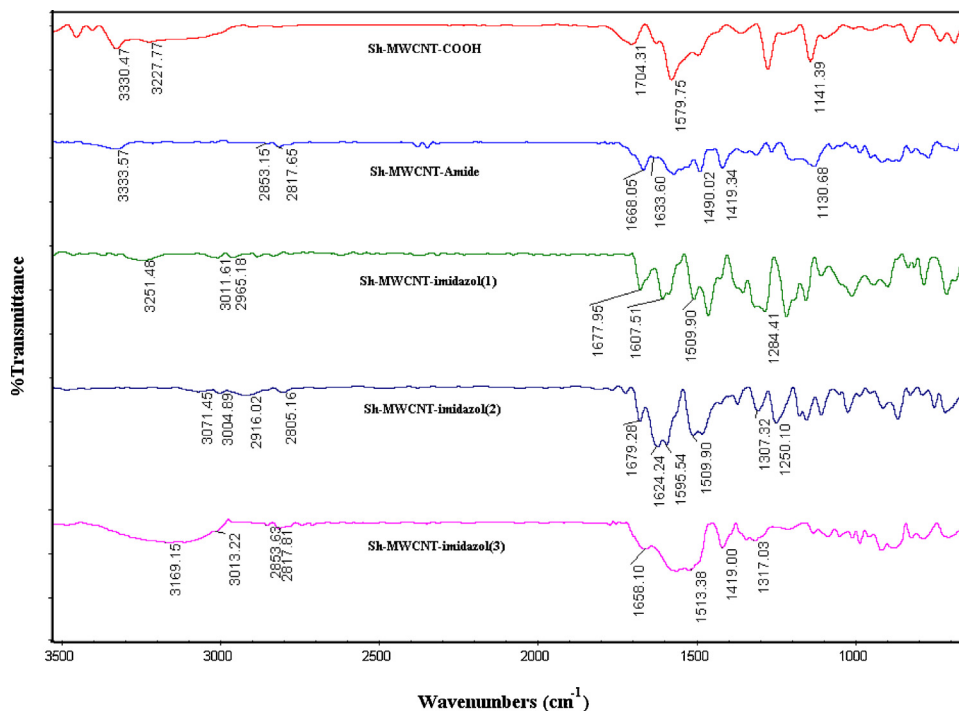

Fig. 3. FTIR spectra (after baseline corrections) of modified Sh–MWCNTs.

tion peaks at 1704 (C=O) and 1141 (C–O) cm^{-1} in the IR spectra of Sh–MWCNT–COOH clearly indicates the presence of carboxylic groups on the Sh–MWCNTs [13]. The two bands at around 2800–3000 that can be seen in all spectra can be related to the C–H stretching of Sh–MWCNTs defects. In the spectrum of Sh–MWCNT–amide, the two peaks at 1668 and 1633 cm^{-1} can be assigned to the amide groups [C(=O)NH linkage] and C=O of
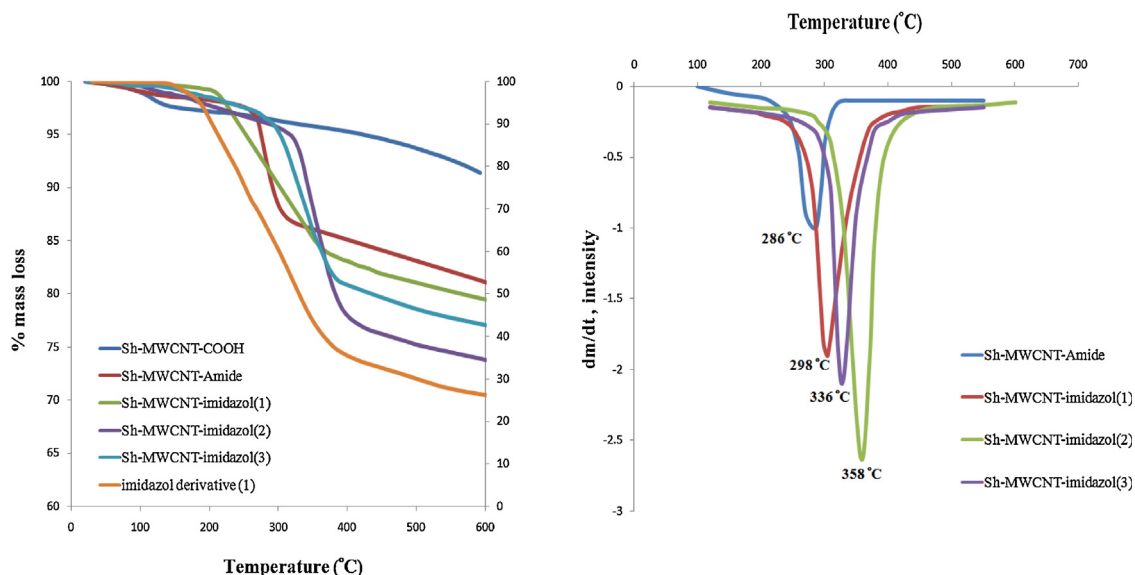
Fig. 4. TGA (a) and DTG (b) curves of modified-MWCNTs under N_2 (10 °C/min). Color available on the web.
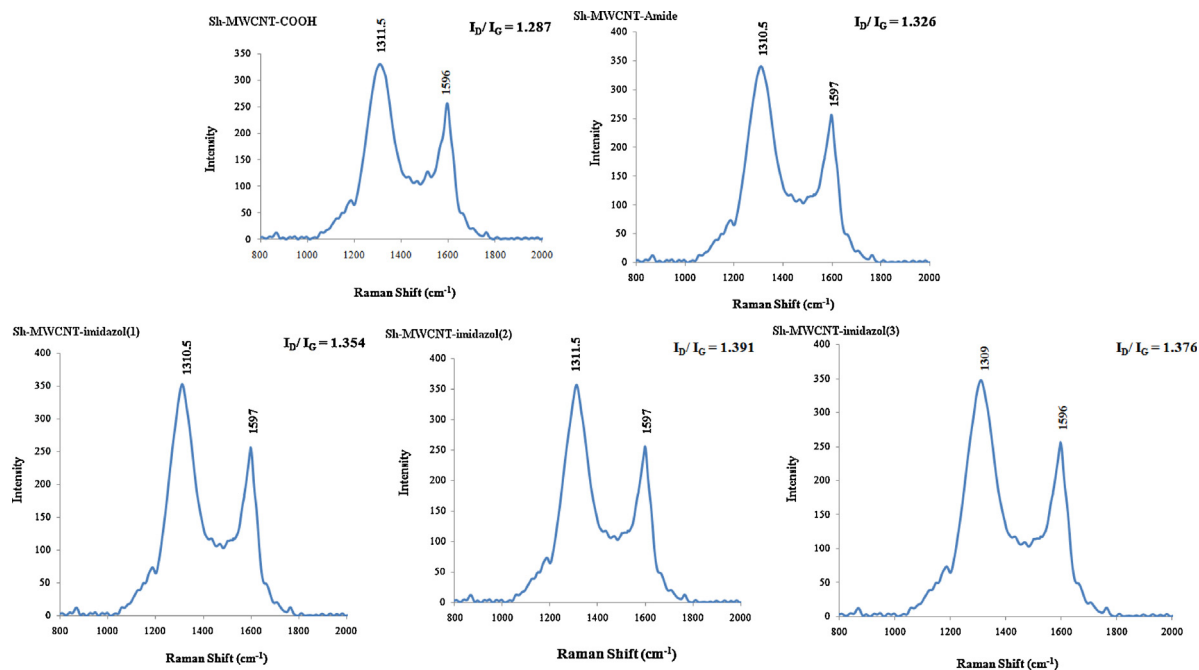

Fig. 5. Raman spectra of modified Sh–MWCNTs. The baseline was corrected for the luminescence background.

creatinine, respectively (as compared to 1704 cm^{-1} for Sh–MWCNTs–COOH), which confirmed the formation of Sh–MWCNT–amide. In the spectra of Sh–MWCNT–imidazols **1**–**3**, the new peaks at around 1600–1630 cm^{-1}, which can be related to the C=C stretching mode of the alkene, confirmed the formation of imidazol derivatives on the CNTs. Also, the peaks at 1677 [Sh–MWCNT–imidazol (**1**)], 1679 [Sh–MWCNT–imidazol (**2**)] and 1658 [Sh–MWCNT–imidazol (**3**)] cm^{-1} can be assigned to the presence of an amide carbonyl. The peaks at around 3300–3600, 1450–1600, 1200–1400 and 1000–1100 cm^{-1} correspond to N–H or OH stretching modes, C=C nanotube, C–N and

C–O stretching modes, respectively. Thus, the FTIR spectra confirm that Sh–MWCNT–COOH has been successfully modified by imidazol derivatives.

The best evidence for the functionalization of MWCNTs is the thermogravimetric analysis (TGA, DTG) results, which provide quantitative information on nanotube functionalization. Since Sh–MWCNT–COOH are almost thermally stable, as shown in Fig. 4a, the weight loss before Sh–MWCNTs decomposition can be used to estimate by TGA the quantity of the various groups attached to the nanotube. According to Fig. 4a, the TGA graph of Sh–MWCNT–amide displays a gradual trend toward decom-

position from 230 to 360 °C, with a weight loss of about 12% that can be assigned to the creatinine attached to CNT. Also, the TGA curves of Sh–MWCNT–imidazol (**1**), Sh–MWCNT–imidazol (**2**) and Sh–MWCNT–imidazol (**3**) evidence decomposition at around 200–432, 302–422, and 250–400 °C, with a mass loss of about 16.2, 18.7 and 16.7%, respectively, probably originating from the loss of the attached imidazol derivatives to CNT (as compared with the TGA curve of Sh–MWCNT–amide). These results indicate that there is one creatinine group for Sh–MWCNT–amide per 96.3, one imidazol derivative (**1**) for Sh–MWCNT–imidazole (**1**) per 125, one imidazol derivative (**2**) for Sh–MWCNT–imidazol (**2**) per 91.7 and one imidazol derivative (**3**) for Sh–MWCNT–imidazol (**3**) per 113 carbon atoms of Sh–MWCNT, respectively, at 422 °C. For example, Fig. 5a compares the TGA curves of the imidazol derivative (**1**) and of Sh–MWCNT–imidazol (**1**).

Fig. 4b shows the DTG curve with respect to temperature for the mass loss curves seen in Fig. 4a. This curve can be used to determine the decomposition temperature of the carbon nanotube, as well as to define the mass loss event as a single decomposing species (e.g., a single peak) or as multiple decomposition events (e.g., double peak, shouldered peaks). The decomposition temperature for each material is defined as the temperature at the highest peak for the material on the DTG curve and can represent further evidence of covalent modification of MWCNTs.

According to Fig. 4b, the major peaks at 286, 298, 358 and 336 °C could be attributed to the loss of the creatinine, imidazol (**1**), imidazol (**2**) and imidazol (**3**) derivatives, respectively bonded to MWCNT. Overall, these results successfully confirm the functionalization of Sh–MWCNT–COOH with these compounds.

The Raman spectra of functionalized MWCNTs (Fig. 5) showed a slight increase of the D-band at $\sim 1310 \text{ cm}^{-1}$; it is attributed to the defects and disorder-induced peaks, relative to the G-band ($\sim 1600 \text{ cm}^{-1}$), which originates from the in-plane tangential stretching mode of carbon–carbon bonds [22], ($I_D/I_G = 1.326–1.397$) compared to Sh–MWCNT–COOH ($I_D/I_G = 1.287$). This indicates a partial destruction of the conjugation structure of the Sh–MWCNTs. In other words, this indicates covalent functionalization of carbon nanotubes by imidazol derivatives attached to the carbon nanotube sidewall [12,13]. It is interesting to note that the largest I_D/I_G ratio is obtained for Sh–MWCNT–imidazol (**2**), which also showed the largest mass loss in the TGA curve.

The toxic effect of functionalized Sh–MWCNTs on gastric and breast cancer cells was investigated. The used biological data in this study revealed some anti-cancer activity against MKN45 and MCF7. Fig. 6 showed images of cell culture on modified Sh–MWCNTs and on control. The figures show targeting of cancerous cells by CNTs, in particular gastric cells. Figs. 6A and G, related to the culture of cancerous cells
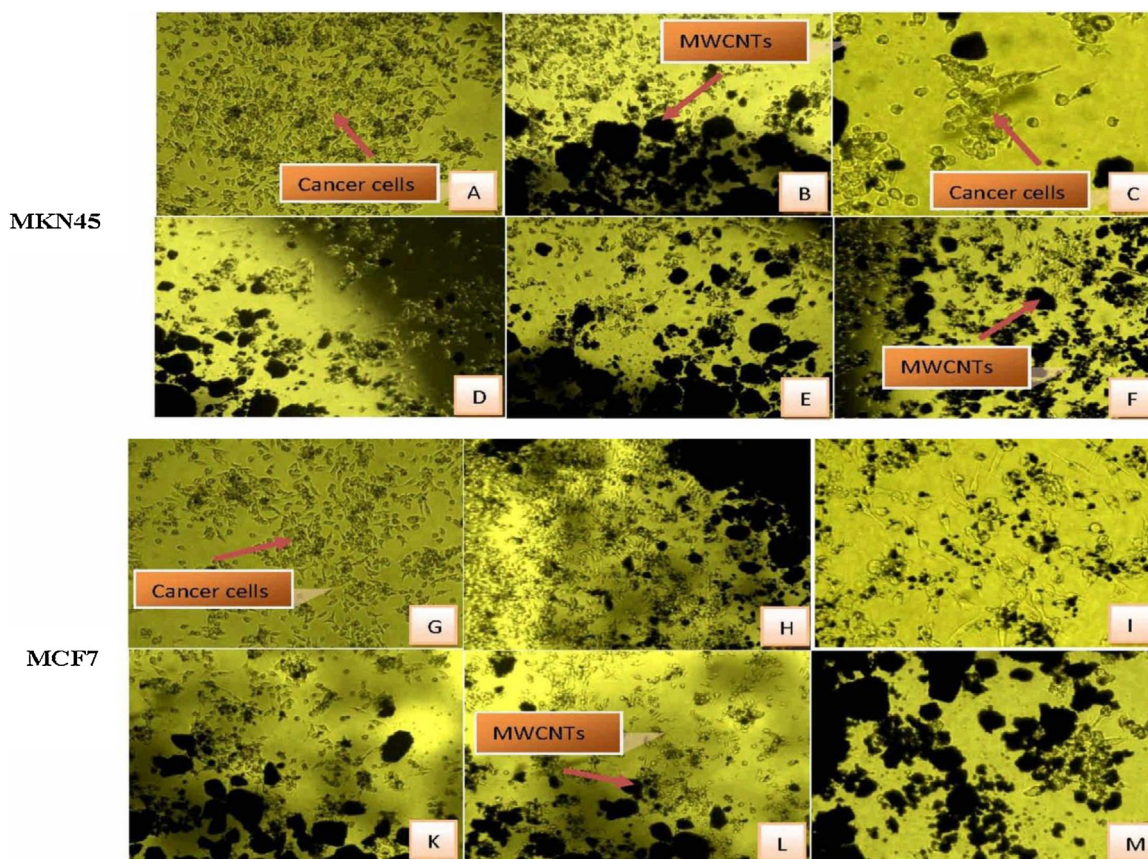

Fig. 6. Cell growth on the samples. Control (A, G), Sh–MWCNT–COOH (B, H), Sh–MWCNT–amide (C, I), Sh–MWCNT–imidazol (**1**) (D, K), Sh–MWCNT–imidazole (**2**) (E, L) and Sh–MWCNT–imidazole (**3**) (F, M). Color available on the web.
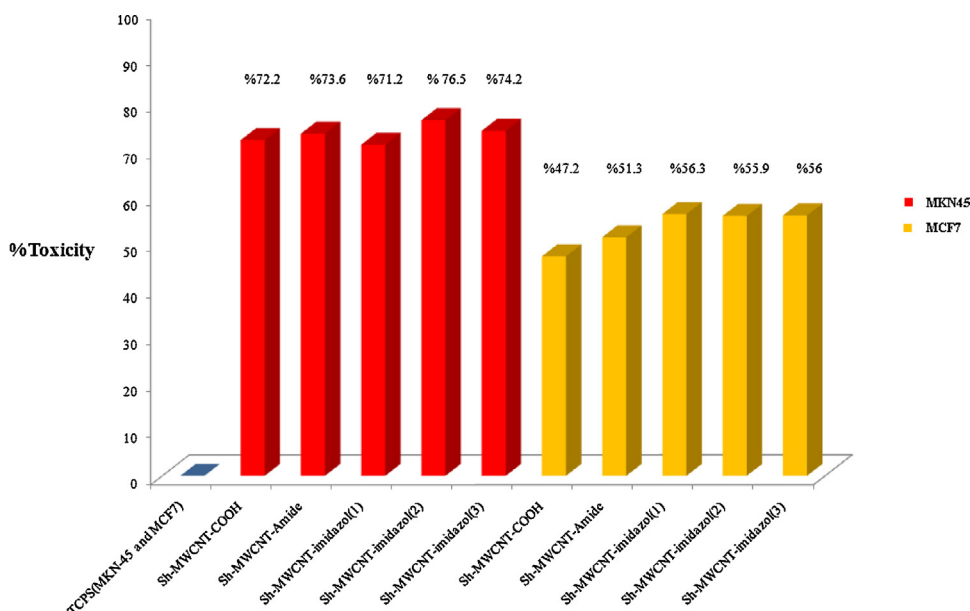
Fig. 7. MTT assay for TCPS and modified Sh–MWCNTs after 72 h. Color available on the web.

on the tissue culture polystyrene (TCPS) surface, show good cell adhesion and proliferation on the TCPS surface. Figs. 6B–F and H–M show the effect of modified Sh–MWCNTs on cancerous gastric and breast cells (respectively, in the vicinity of the modified Sh–MWCNTs and the control sample). These results show that the modified Sh–MWCNTs diffuse well into and on cancerous cells.

Fig. 7 shows an MTT assay for TCPS (control), Sh–MWCNT–COOH, Sh–MWCNT–amide and Sh–MWCNT–imidazols **1**–**3** on MKN45 and MCF7. The results showed the high toxicity of modified-MWCNTs for MKN45 (about 71–77%) compared to MCF7 (about 47–56%). Also, the toxicities of functionalized Sh–MWCNTs in MCF7 and MKN45 are approximately similar. We dictated for which concentration the samples could be considered similar (100 μg/mL). Overall, these results demonstrated that modified Sh–MWCNTs are a powerful agent for MKN45, compared to MCF7, which kills cancer cells at a rate of about 71–77%.

4. Conclusion

We have firstly introduced imidazol derivative groups on the surface of carbon nanotubes via thermal and microwave methods; the obtained results showed that the latter were similar. The reported results demonstrated the functionalization of Sh–MWCNT–COOH by imidazol derivatives. Also, the modified Sh–MWCNTs can potentially be used as cellular killers, especially of cancerous cells. Our results demonstrated the higher toxicity of modified Sh–MWCNTs toward gastric cancer cells (71–77%) compared to breast cells (47–56%).

References

[1] A. Merkoc, Microchim. Acta 152 (2006) 157.
[2] S. Reich, C. Thomsen, J. Maultzsch, Carbon Nanotubes, Wiley–VCH, Berlin, 2010.
[3] C. Klumpp, K. Kostarelos, M. Prato, A. Bianco, Biochim. Biophys. Acta 1758 (2006) 404.
[4] S. Iijima, Nature 354 (1991) 56.
[5] P.L. McEuen, M.S. Fuhrer, H. Park, IEEE Trans. Nanotech. 1 (2002) 78.
[6] T. Durkop, S.A. Getty, E. Cobas, Nano Lett. 4 (2004) 35.
[7] D. Pantarotto, R. Singh, D. McCarthy, M. Erhardt, J.-P. Briand, M. Prato, Angew. Chem. Int. Ed. 43 (2004) 5242.
[8] A. Bianco, K. Kostarelos, M. Prato, Curr. Opin. Chem. Bio. 9 (2005) 674.
[9] M. Popławska, G.Z. Zukowska, S. Cudziło, M. Bystrzejewski, Carbon 48 (2010) 1312.
[10] F. Cataldo, Fullerenes, Nanotubes, Carbon Nanostruct. 16 (2008) 1.
[11] A. Heidari, M.H. Beheshty, H. Rahimi, Fullerenes, Nanotubes, Carbon Nanostruct. 21 (2013) 516.
[12] H. Tahermansouri, Y. Aryanfar, E. Biazar, Bull. Korean Chem. Soc. 34 (2013) 149.
[13] H. Tahermansouri, M. Azadfar, S. Heidari, Fullerenes, Nanotubes, Carbon Nanostruct. 21 (2013) 568.
[14] J. Azizian, H. Tahermansouri, D. Chobfrosh khoei, K. Yadollahzadeh, A.S. Delbari, Fullerenes, Nanotubes, Carbon Nanostruct. 20 (2012) 183.
[15] J. Azizian, D. Chobfrosh Khoei, H. Tahermansouri, K. Yadollahzadeh, Fullerenes, Nanotubes, Carbon Nanostruct. 19 (2011) 753.
[16] J. Azizian, H. Tahermansouri, E. Biazar, S. Heidari, D. Chobfrosh Khoei, Int. J. Nanomed. 5 (2010) 907.
[17] H. Tahermansouri, D. Chobfrosh Khoei, M. Meskinfam, Orient. J. Chem. 27 (2011) 499.
[18] H. Tahermansouri, M. Atghaee, M. Azadfar, Orient. J. Chem. 27 (2011) 1325.
[19] O. Moradi, M. Yari, K. Zare, B. Mirza, F. Najafi, Fullerenes, Nanotubes, Carbon Nanostruct. 20 (2012) 138.
[20] A. Aqel, K.M.M. Abou El-Nour, R.A.A. Ammar, A. Al-Warthan, Arab. J. Chem. 5 (2012) 1.
[21] E. Vázquez, M. Prato, ACS Nano. 3 (2009) 3819.
[22] H. Hiura, T.W. Ebbesen, K. Tanigaki, Chem. Phys. Lett. 202 (1993) 509.